MOLECULAR IMAGING AND BIOLOGY

Mol Imaging Biol (2013) 15:423–430
DOI: 10.1007/s11307-013-0614-2

Published Online: 2 February 2013

World Molecular Imaging Society

RESEARCH ARTICLE

Evaluation of Inflammatory Response to Acute Ischemia Using Near-Infrared Fluorescent Reactive Oxygen Sensors

Selena Magalotti,[1] Tiffany P. Gustafson,[1] Qian Cao,[1] Dana R. Abendschein,[2] Richard A. Pierce,[2] Mikhail Y. Berezin,[1] Walter J. Akers[1]

[1]*Department of Radiology, Washington University School of Medicine, St. Louis, MO, 63110, USA*
[2]*Department of Internal Medicine, Washington University School of Medicine, St. Louis, MO, 63110, USA*

Abstract

Purpose: Ischemia-related processes associated with the generation of inflammatory molecules such as reactive oxygen species (ROS) are difficult to detect at the acute stage before the physiologic and anatomic evidence of tissue damage is present. Evaluation of the inflammatory and healing response early after an ischemic event *in vivo* will aid in treatment selection and patient outcomes. We introduce a novel near-infrared hydrocyanine molecular probe for the detection of ROS as a marker of tissue response to ischemia and a precursor to angiogenesis and remodeling. The synthesized molecular probe, initially a non-fluorescent hydrocyanine conjugated to polyethylene glycol, converts to a highly fluorescent cyanine reporter upon oxidation.

Procedures: The probe was applied in a preclinical mouse model for myocardial infarction, where ligation and removal of a portion of the femoral artery in the hindlimb resulted in temporary ischemia followed by angiogenesis and healing.

Results: The observed increase in fluorescence intensity was approximately sixfold over 24 h in the ischemic tissue relative to the uninjured control limb and was attributed to the higher concentration of ROS in the ischemic tissue.

Conclusions: These results demonstrate the potential for non-invasive sensing for interrogating the inflammatory and healing response in ischemic tissue.

Key words: Cardiovascular disease, Optical imaging, Activatable, Hindlimb ischemia, Molecular imaging

Introduction

Angiogenesis, the process of reperfusion *via* the budding of new capillaries from nearby existing vessels, is essential for recovery from myocardial infarction (MI) [1, 2]. Non-invasive monitoring of the healing process in a clinical setting is highly desired. It would offer a method to stage recovery and individualize follow-up care after any type of acute MI [3]. Current imaging modalities measure anatomic (CT, MRI), functional (echocardiography), or perfusion (SPECT/PET) changes to assess healing after ischemic damage [3]. These clinical modalities lack sensitivity to early molecular signatures of damage and the healing response, although new contrast agents are being investigated [3]. Detection of molecular events that signal positive or negative healing responses would greatly benefit treatment of patients with cardiovascular disease.

Selena Magalotti and Tiffany P. Gustafson contributed equally to this study.

Electronic supplementary material The online version of this article (doi:10.1007/s11307-013-0614-2) contains supplementary material, which is available to authorized users.

Correspondence to: Mikhail Berezin; *e-mail:* berezinm@mir.wustl.edu, Walter Akers; *e-mail:* akersw@mir.wustl.edu

Accumulated evidence suggests that reactive oxygen species (ROS) in ischemia reperfusion mediate a variety of growth-related responses including angiogenesis [4, 5]. A number of chemical factors are released upon vascular injury that can attract macrophages to the site of damage [6]. As a result, macrophages play a critical role in the early stages of angiogenesis. They are involved in production of cytokines which draw angiogenic precursors to break down extracellular matrix (ECM) and release ECM-embedded factors such as VEGF which stimulates formation of new capillaries [5]. A fundamental component of macrophage physiology is the release of ROS *via* the "respiratory burst" [5, 7]. A high concentration of these species immediately after injury has been confirmed in both animal models and human tissues [5]. We hypothesized that the level of ROS in the affected tissue correlates with the inflammatory and angiogenic processes, thus providing a surrogate marker for early assessment of the healing process after MI.

Fluorescent probes which detect ROS have long been utilized for studying oxidative processes in cell-based microscopy and enzymatic assays. Recently, near-infrared hydrocyanine probes ("OFF–ON" dyes) have been reported as sensors for ROS *in vitro* and *in vivo* [8–10]. The concept of this approach is based on the following: in the reduced protonated form, the conjugated electron system of the hydrocyanine is separated by an sp^3 carbon forming a colorless and, hence, non-fluorescent ("OFF") form of the dye. Upon oxidation and deprotonation, all cyanine carbons regain sp^2 hybridization, the conjugated system is restored, and the molecule recovers fluorescence ("ON"). In the work described herein, a novel hydrocyanine-based construct for detection of ROS in an animal model of MI is reported. The construct is composed of a hydrocyanine dye covalently conjugated to a medium-length polyethylene glycol (PEG) to prolong circulation time and increase the opportunity for oxidation. The ROS sensor construct was evaluated in a small animal ischemia model.

Results

Probe Design

The developed ROS probe was comprised of the hydrocyanine form of the recently reported polymethine dye LS601 [11, 12] conjugated to a 40 kD PEG (PEG_{40}). LS601 exhibits increased hydrophilicity and low albumin binding [11], minimizing non-specific protein interactions [12]. To verify that the hydrocyanine form of a free dye is sensitive to ROS, the fluorescent dye was reduced to its non-fluorescent counterpart LS601R (R stands for reduced) *via* treatment with sodium borohydride ($NaBH_4$) [13] (Scheme 1). The reaction was monitored by UV/Vis, following the loss of absorbance at ~750 nm and the appearance of a new absorption peak at ~400 nm which corresponds to the shortened conjugation system. Oxidation of LS601R with Fenton reagent led to recovery of LS601 and restoration of fluorescence (Fig. S1).

Having verified the sensitivity of LS601R to ROS, LS601 was preactivated as an *N*-hydroxysuccinimide (NHS) ester and reacted with methoxy-PEG_{40}-amine under standard NHS coupling conditions (Scheme 2). The conjugate, LS601-PEG_{40}, was purified *via* gel filtration chromatography; the fractions were collected and analyzed *via* fluorescence anisotropy and SDS-PAGE to select the fractions with the highest purity of the product.

Fluorescence anisotropy was used to identify the fractions with minimum amount of the free dye. The method distinguishes high molecular weight conjugated dye from its free form based on the relative rotational velocity of the molecules in solution [14]. Placement of the activatable carboxylic functionality as part of the dye's core ensures minimal independent motion of the probe after conjugation, allowing for utilization of fluorescence anisotropy to monitor the coupling process. We have previously demonstrated that in its free form, the dye anisotropy value is relatively low (~0.24), yet in an immobile state (glycerol, 4 °C), the dye exhibits a limiting anisotropy of ~0.37 [12]. The values for conjugates depend on the molecular weight and shape of the macromolecule. Since the fluorescence anisotropy is inherently additive, this value has a direct correlation to the purity of the conjugate—free dye contributes to a lower value of fluorescence anisotropy. Based on this rationale, fractions with anisotropy values from 0.28 to 0.31 were selected for SDS-PAGE analysis.

As LS601 contains two symmetrical functional groups for conjugation, collected fractions were further characterized by SDS-PAGE to quantify conjugation and identify the fractional composition as *mono* or *bis* product formed during the coupling reaction (Fig. 1a). Based upon analysis of the fluorescence intensity of bands from the fractions selected by anisotropy method, the fluorophores were primarily the result of *mono* ~70 % and *bis* ~22.5 % addition. Remaining ~7.5 %

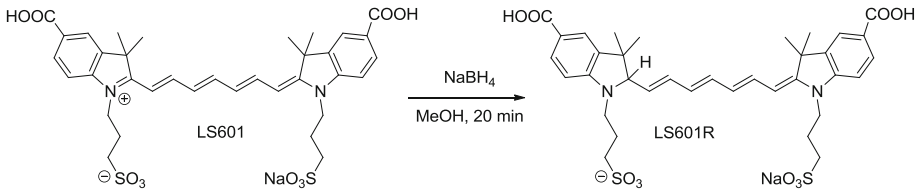

Scheme 1. Reduction of fluorescent LS601 to its non-fluorescent hydrocyanine form LS601R.

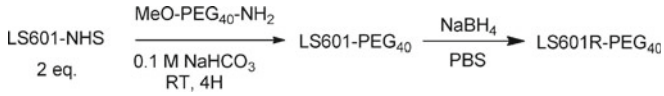

Scheme 2. Synthesis of LS601R-PEG_{40} conjugate.

corresponded to a free dye. These fractions were isolated and converted to the ROS probe.

LS601-PEG_{40} was redissolved in PBS buffer and reduced with $NaBH_4$ to obtain LS601R-PEG_{40} conjugates. The reduction appeared complete, with no residual starting material observed as judged by UV/Vis spectroscopy (Fig. 1b) and absence of fluorescence. The resulting "OFF" construct was expected to have similar reactivity with ROS as compared to the free probe and, thus, was used directly for animal studies without *in vitro* testing.

Animal Studies

Biodistribution of the "ON" LS601-PEG_{40} Probe in the Hindlimb Ischemia Model

A control, always "ON" fluorescent LS601-PEG_{40}, was injected into a hindlimb ischemia model to assess the longitudinal distribution of the dye. Fluorescence imaging data were analyzed using regions of interest (ROI) selected for the distal thigh of the injured and uninjured control limbs. Immediately after probe injection, the fluorescence intensities at both limbs were similar (Figs. 2 and 3). As expected for the healthy tissue, the fluorescence intensity decreased over time in the uninjured limb. This decrease was relatively slow due to the long circulation time of the high molecular weight contrast agent. In contrast, the fluorescence intensity in the injured limb increased over the first 4 h with further modest increase between 4 and 24 h. The elevation in intensity (~2×) can be explained by the enhanced vascular permeability resulting from post-ischemic inflammation and, therefore, the reduced clearance of the agent from the injured tissue. Although the "ON" LS601-PEG_{40} can be utilized for evaluating the physical status of vascular membranes, it does not provide information on the molecular status of the healing process. In fact, the large experimental error seen in the injured group demonstrates the biological variability in the healing response between individuals that would be difficult to detect using other methods.

Biodistribution of the "OFF" Probe LS601R-PEG_{40} Indicates Inflammation

The hydrocyanine "OFF" probe LS601R-PEG_{40} was administered to mice under the same conditions as the "ON" LS601-PEG_{40}. In contrast to the previous experiment with "ON" LS601-PEG_{40} probe, immediately after injection of the LS601R-PEG_{40}, the fluorescence intensities at both limbs were several orders of magnitude lower. In the uninjured limb, the fluorescence immediately after intravenous administration of LS601R-PEG_{40} and 24 h later was equivalent to the pre-injection values (Fig. 4). Meanwhile, the fluorescence intensity from the distal thigh of the injured limb increased dramatically after injection with the highest measured intensity, almost sixfold higher than post-injection, occuring at 24 h post-injection (Fig. 4). This result suggests both activation of the probe due to post-ischemic ROS detection of inflammation and possible accumulation of the probe at the site of injury due to the enhanced permeability and retention effect.

The progressive increase in fluorescence intensity with LS601R-PEG_{40} in the ischemic hindlimb allows visualization of ROS in the ischemic tissue. Interestingly, the experimental error was much lower for these groups than for the LS601-PEG_{40} groups, indicating that the angiogenic response is not directly correlated with vascular permeability. Further study is warranted to evaluate the connections between ROS and angiogenesis.

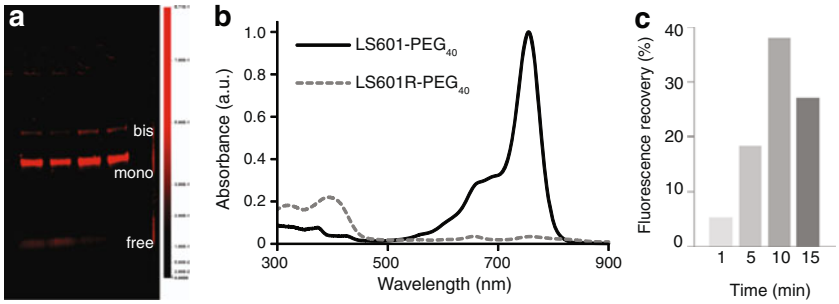

Fig. 1. **a** SDS-PAGE gel for fractions collected from purification of the reaction mixture using a Sephadex G25 column (λ_{ex}= 785 nm, λ_{em}=810 nm). Based on the location on the gel, the bands indicate the makeup of the product to be free LS601 7.5 % (*bottom band*), *mono* LS601-PEG_{40} 70.0 % (middle band), and *bis* LS601-PEG_{40}; 22.5 % (*top band*); **b** UV/Vis spectra of LS601-PEG40 before and after reduction in PBS buffer. **c** Representative graphical comparison of percent increase in fluorescence intensity over time following addition of Fenton's reagent to LS601R. This decrease in fluorescence after 10 min was attributed to subsequent over-oxidation of the fluorophore at high oxidative stress.

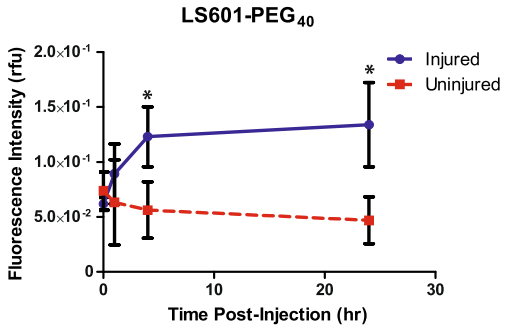

Fig. 2. Fluorescence intensity (in relative fluorescence units) for ROIs selected from the lower limbs of mice at given timepoints after intravenous injection of LS601-PEG_{40} (n=3 mice). Based upon our results (see Results section), which indicate the free dye clears from injured control animals within 4 h, attachment to PEG_{40} does result in significantly higher circulation times within which detection of ROS could take place. The fluorescence intensity increased about twofold in the injured limb over 24 h. *Bars* indicate standard deviation, and *single asterisk* (*) indicates statistically significant (P<0.01) differences.

Histology Confirmed Tissue Oxidation

Among ROS, oxygen superoxide O_2^-, hydrogen peroxide (H_2O_2), and hydroxyradical ($OH^\bullet$) are the most prevalent species. These molecules are highly reactive in biological tissues (residence time less than several seconds [15]) and rapidly participate in protein, lipid, and RNA/DNA oxidations leading to the formation of other active species such as peroxynitrite ($ONOO^-$, a product of reaction between a superoxide O_2^- and nitric oxide NO).

Increased levels of oxidation products at the site of injury are commonly assessed *ex vivo via* immunohistochemistry for specific markers such as 8-hydroxy-deoxyguanosine (8-OHG, reflecting nucleic acid modifications) and nitrotyrosine (reflecting protein nitration with peroxynitrite). Under oxidative stress, the DNA and RNA deoxyguanosine transforms into its oxidized analog 8-OHG; while tyrosine, upon reaction with peroxynitrite, is converted into its nitrotyrosine form. With known antibodies against 8-OHG and nitrotyrosine, normal tissue is clearly distinguished from the injured. Positive staining distal to the injury for these markers was used to confirm oxidative stress in the tissue and the macrophage's role in angiogenesis in the hindlimb ischemia model.

Specimens of the thigh muscles from both control and ischemic hindlimbs were cut into 10-µm sections and stained for 8-OHG and nitrotyrosine. Staining for 8-OHG showed a mild increase in the level of oxidized DNA in the injured limbs relative to the non-injured controls (Fig. 5). Staining with anti-nitrotyrosine antibody also showed a mild increase in protein oxidation in the injured limbs (Fig. 6 and Fig. S2). These mild changes in oxidation on histology correspond to the modest increase in fluorescence intensity for LS601R-PEG_{40} in the injured *versus* control hindlimb (Fig. 3).

Discussion

The extent of ischemic injury which occurs due to events such as coronary blockage is an important prognostic indicator for recovery [1, 2]. After ischemia, inflammation occurs, including invasion of macrophages and subsequent release of cytokines and ROS that induce the process of angiogenesis. Methods that enable evaluation of the inflammatory response will better enable full characterization of the extent of injury and therapeutic interventions. We hypothesized that fluorescent dyes sensitive to ROS concentration would enable detection of ischemia-induced inflammatory response in muscle tissues relative to healthy muscle. To this purpose, long-circulating NIR fluorescent hydrocyanine molecular probes were developed and tested in a mouse model of ischemic injury.

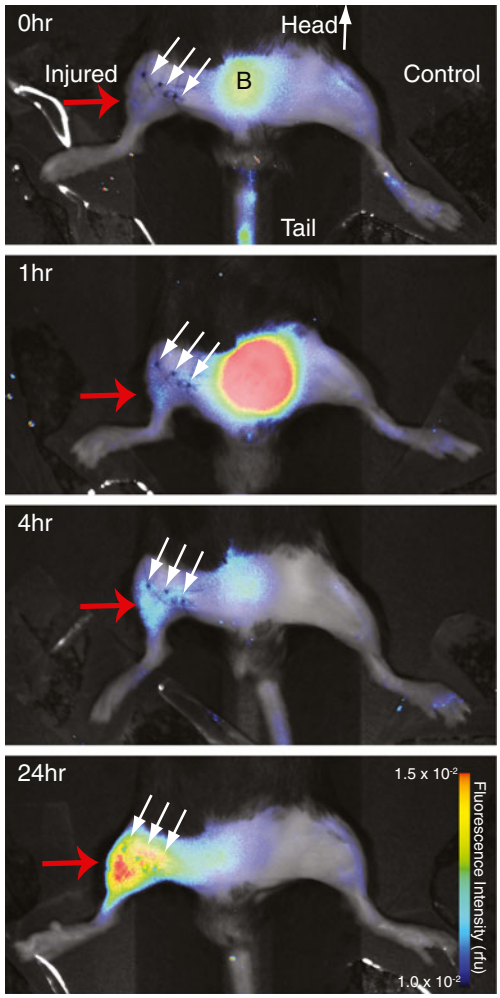

Fig. 3. Fluorescence intensity imaging of a mouse at 0, 1, 4, and 24 h after injection of LS601R-PEG_{40} (λ_{ex}=785 nm, λ_{em}=810 nm). *Small arrows* show the line of surgical incision, region B corresponds to bladder. Fluorescence increased an average of 5.8 times the post-injection values in the distal thigh of the injured limbs (*red arrow*) resulting from ROS detection at the site of ischemia. Fluorescence in the uninjured limbs was not significantly different (P>0.05) at different timepoints.

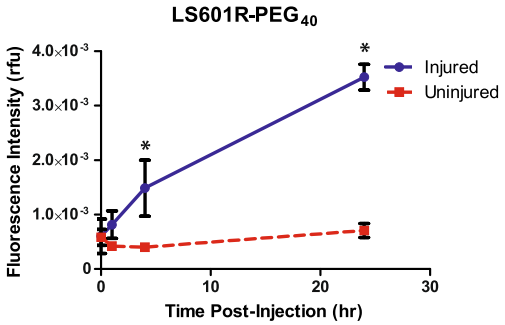

Fig. 4. Fluorescence intensity (in relative fluorescence units) for ROIs selected from the lower limbs of mice at given timepoints after intravenous injection of LS601R-PEG$_{40}$ (n=3). *Bars* indicate standard deviation, and *single asterisk* (*) indicates statistically significant (P<0.01) differences.

Induction of ischemia in the hindlimb of mice by transection of the femoral artery is a favorable model for the study of ischemic injury and healing [16]. Following total excision of the femoral artery, it takes 28 days for the muscles to regain normal perfusion *via* expansion of collateral circulation [17]. We hypothesized that after tissue ischemia and before evident angiogenesis, the ROS levels would be increased as a result of post-injury inflammatory processes which includes infiltration of the tissue by macrophages and other leukocytes. A simple method for detection of ROS would enable non-invasive visualization of the disease and potentially provide an ample timeframe to study the effects of medical intervention on the process of angiogenesis and tissue healing [16].

The use of LS601 for coupling to targeting moieties [12] and imaging *in vivo* [11] has recently been reported. This NIR dye

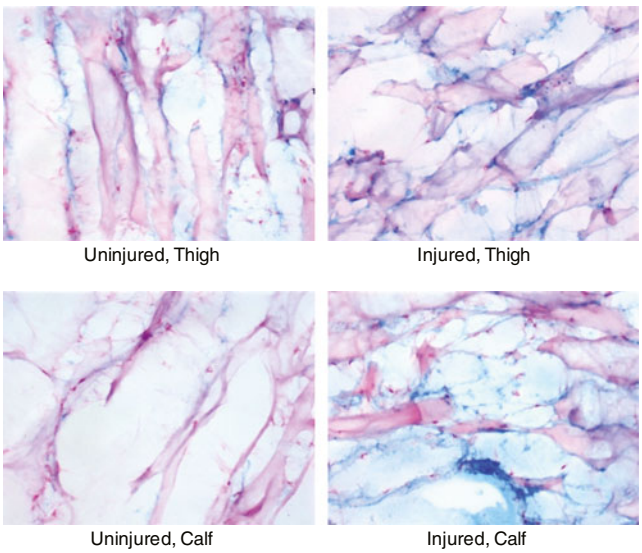

Fig. 5. Muscle tissues were stained for 8-OHG (*blue*), which can be located in RNA or DNA structure. The blue staining in the muscle specimens appeared non-cellular and, therefore, either non-specific or representing extracellular debris from dead cells. Few nuclei (*pink*) are present in the muscle specimens though the muscle itself took up eosin counterstain.

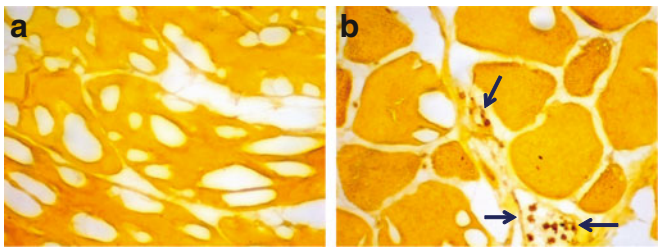

Fig. 6. Immunohistochemistry of thigh muscle tissue for nitrotyrosine. Positive signal is *brown*, and the counterstained tissue is *yellow-orange*. **a** Control thigh muscle shows little evidence of nitrotyrosine. **b** Ischemic thigh muscle shows positive staining in inflammatory cells (*arrows*) within and around small intramuscular blood vessels. Results are representative for healthy and ischemic tissues from n=4 subjects, including those represented in Fig. 4. Additional images are shown in Fig. S2.

has favorable optical properties, including high brightness and a relatively long fluorescent lifetime (Table 1). It also has excellent chemical qualities such as chemical stability and high coupling efficiency to macromolecules [12]. We have shown in this study that reduction of LS601-PEG to its hydrocyanine form is effective in the detection of ROS produced by inflammatory cells attracted to an area of ischemia. Further, the "OFF" version of this dye reported the presence of oxidative stress *in vivo* (Fig. 3). As redox reactions are diffusion controlled and, therefore, slow relative to the clearance of small, hydrophilic dyes, the reporter was attached to a non-immunogenic, biocompatible macromolecule, methoxy-PEG$_{40}$-amine to increase circulation time. The use of this larger construct allowed for retention of the probe in acutely injured tissues as a result of increased vascular permeability [18]. The LS601-PEG$_{40}$ construct retained hydrophilicity and preferred renal elimination route as indicated by high fluorescence from the bladder region in Fig. 3. Renal elimination of LS601-PEG$_{40}$ and LS601R-PEG$_{40}$ conforms to previous observations that linear polymer constructs pass through the glomerulus while globular polymers do not [19, 20].

Myocardial infarction is a serious disease in which the true extent of injury often cannot be ascertained through anatomical and functional assessment and requires a "wait and see" approach. Early staging of the disease using ROS sensing could provide greater insight to the extent of injury, guiding initial therapy and improving patient outcomes. ROS-sensing agents could be advantageous clinically as prognostic indicators of angiogenesis and healing or through

Table 1. Photophysical properties of LS601in DMSO

Dye	λ_{abs} (nm)	λ_{em} (nm)	ε($M^{-1}cm^{-1}$)	Φ	τ (ns)	χ^2
LS601	769	800	161,000	0.20	1.30	1.08

λ_{abs} absorption maximum, λ_{em} emission maximum, ε molar absorptivity at the λ_{abs}, Φ fluorescence quantum yield, τ fluorescence lifetime, χ^2 goodness of fit for two-exponential fit, the major component fraction contribution >96 %

endoscopic imaging visualization. Optical imaging for MI would require endoscopic technologies for visualizing fluorescent signals deep within the body and could be used to pinpoint the exact location of ischemic injury. Such improved techniques for angiogenesis detection *via* the visualization of ROS could permit more precise diagnosis and treatment of ischemic injury after myocardial infarction.

Non-invasive monitoring of ROS also has significant potential to impact clinical management of peripheral ischemic injury and related diseases accessible to currently available and newly developed optical imaging technologies. Planar reflectance imaging utilized in this work enables longitudinal non-invasive imaging over large fields of view for superficial fluorescence measurements [21]. These technologies are being applied for imaging arthritis-related inflammation and for guiding surgical interventions. For diseases deeper in tissues, diffuse optical tomography [22] and photoacoustic tomography [23] enable detection of optical contrast agents as deep as 10 cm below the skin surface. With these technologies, optical imaging with ROS-sensitive molecular probes can be directly applied at the point of care for improved disease assessment and therapeutic decisions.

Summary

Development of fluorescent ROS probes to enable identification of ischemic injury and quantify the extent of angiogenesis could be an invaluable addition to the current imaging modalities for diagnosis, treatment, and monitoring of recovery from MI and/or other types of ischemic injuries. Toward achieving this goal, we have developed novel diagnostic agents for the detection of injury-induced ROS production and tested them in a mouse hindlimb ischemia model. High contrast in the injured tissue as compared to the control non-injured limb demonstrates that the developed ROS probe possesses sufficient sensitivity for *in vivo* detection of low-level oxidative stress. Further investigation to confirm the prognostic importance of ROS levels in post-ischemia tissues for prediction of healing and responses to therapy is underway.

Methods

Synthesis and Characterization

General Information

Common solvents, indocyanine green (ICG), and reagents for synthesis were purchased from Sigma-Aldrich, Alfa Aesar or TCI America and used without further purification. NMR spectra were recorded at room temperature on a Varian 600 MHz instrument, in DMSO with TMS as an internal standard (unless noted otherwise). MilliQ water (Millipore) was used throughout this work. The compounds were analyzed using LC/MS-ESI analysis in the positive mode conducted on a Shimadzu 2010 A LCMS equipped with a UV/Vis detector at different wavelengths using a reversed-phase C-18 Vydac column (218TP, 4.6×50 mm) at a flow rate of 0.7 ml/min with a gradient of 10–95 % acetonitrile in water (both solvents contained 0.1 % TFA).

LS601

Synthesis of LS601 was carried out as previously described [11, 12].

LS601R

LS601 (0.028 mmol) was dissolved in MeOH (7 ml) and put on ice. $NaBH_4$ (0.113 mmol) was added to MeOH (0.5 ml) on ice, and the $NaBH_4$ solution was added drop wise to the dye-methanol solution with stirring. The reaction was monitored by the disappearance of the absorption band at ~780 nm using UV/Vis spectroscopy. The reaction was then warmed to room temperature with stirring over 20 min. The solvent was removed under vacuum to yield the final product.

Oxidation with Fenton Reagent

Oxidation was conducted directly in a quartz cuvette. The cuvette was placed in a fluorometer. From a fresh stock solution of the dye LS601R 1 mg/ml in DMSO, 5 ul was added to 2 ml of methanol in a cuvette. Emission spectrum of the solution was obtained at excitation of 720 nm and an emission range of 735–950 nm. Hydrogen peroxide (15 µl) of the 100 µM stock solution in water was added to the cuvette while stirring the solution with a magnetic stirbar. Ferrous sulfate stock solution (15 µl) of the 10 mM solution in water was added to the cuvette immediately after hydrogen peroxide addition. Readings were taken at 1, 5, 10, and 15 min after addition of the ferrous sulfate.

LS601-NHS Ester

The procedure was followed from Gustafson *et al.* [12]. For LS601 (56 mmol) dissolved in DMF (2 ml), *N*-hydroxysuccinimide (120 mmol) and N-(3-dimethylaminopropyl)-N′-ethylcarbodiimide hydrochloride (EDC, 120 mmol) were added at once, and the reaction mixture was stirred overnight at room temperature. Diethyl ether (10 ml) was added to the reaction mixture to precipitate the product. The obtained precipitate was re-dissolved in a minimal amount of methanol and further precipitated with ether; precipitation was repeated again to give the desired NHS ester as green solid (47 mg, 52 mmol, 92 % yield). MALDI-MS *m/z*: 907 [M^+, *bis*-NHS], 810, [M^+, *mono*-NHS]. ESI-MS *m/z*: 908 [M^+, *bis*], 811 [M^+, Mono].

LS601-PEG$_{40}$

Methoxy-PEG-amine with molecular weight 40 kD (2.5 µmol) was dissolved in 0.1 M $NaHCO_3$ buffer (1 ml). LS601-NHS ester (5 µmol) was dissolved in DMSO (100 µl) and added to the PEG solution. The reaction mixture was left shaking at room temperature for 3 h. The conjugate was purified on a Sephadex G-25 column and eluted with water. Fractions were evaluated by fluorescence anisotropy and SDS-PAGE. Selected fractions containing product at the highest concentrations were collected and lyophilized to provide 30 mg of the conjugate.

LS601R-PEG$_{40}$

LS601-PEG$_{40}$ (0.28 μmol) was dissolved in water (1 ml) and put on ice. $NaBH_4$ (20 μl of 1 mg/ml solution in water) was added to the PEG solution in 5 μl increments while monitoring by UV/Vis at 20 °C. Following addition of 20 μl $NaBH_4$, UV/Vis indicated that all dyes have been reduced (Fig. 1). The reaction was protected from light overnight before *in vivo* use.

Optical Measurements

UV/Vis spectra of samples were recorded on a Beckman Coulter DU 640 UV/Vis spectrophotometer. Steady-state fluorescence spectra, fluorescence lifetime, and anisotropy were recorded on a Fluorolog-3 spectrofluorometer (Horiba Jobin Yvon, Inc.). The photophysical data (steady-state absorption, fluorescence) and lifetime were obtained in DMSO and water. Fluorescence quantum yield of the probe was measured using relative method with ICG as a standard [24]. Fluorescence lifetime of dyes was determined using time-correlated single photon counting technique with NanoLed 700 or 773-nm excitation source as described previously [25]. Fluorescence anisotropy was measured as described previously [12].

SDS-PAGE

An SDS-PAGE was run for each conjugate using a Bio-Rad Any KD or 4–20 % Mini-PROTEAN® TGX™ Gel according to the manufacturer protocol (Bio-Rad Laboratories). A Precision Plus Protein All Blue Standard, fluorescent at 710 nm, was used as the ladder (Bio-Rad). The gel was imaged using the Pearl Imager NIR fluorescence small animal imaging system (Li-COR, Lincoln, NE, USA), with excitation at two different wavelengths 685 and 785 nm and corresponding emission collected at 710 and 810 nm, respectively. Three prominent bands corresponding to the free dye (MW <1,000), *mono* (MW ~41,000), and *bis* substituted LS601-PEG$_{40}$ (MW ~82,000) were identified based on the position of the bands relative to the ladder. Quantitative analysis of the gel was carried out using Pearl Cam Software (Li-COR). An equal size region of interest (ROI) was drawn around each band of the gel, within each channel, and the mean intensity for each ROI was measured, and the background subtracted. Relative contribution (A_i) of each band was calculated from fluorescence intensities (F) according to Eq. 1

$$A_i = \frac{F_i}{F_{dye} + F_{mono} + F_{bis}} \times 100\ \% \qquad (1)$$

Animal Studies

All animal studies were conducted in accordance to protocols approved by the Washington University Animal Studies Committee.

Surgical Procedure

Ischemia was induced in the mouse hindlimb through unilateral excision of a segment of the right femoral artery in 6–10-week-old C57B16 black male mice (Harlan) using the technique adapted from previously described methods [17, 26]. Mice were anesthetized using 2 % isoflurane at 1 l/min, and a surgical plane was verified by absence of a toe pinch reflex. Buprenorphine (0.1 mg/kg) was administered subcutaneously before surgery and again 12 h post-surgery. Hair was removed from lower abdomen and ventral surface of both hindlimbs using gentle electric clipping and cream depilatory. Mice were positioned supine on a covered heating pad, and the limbs secured. The right hindlimb was prepped for aseptic surgery by application of betadine and ethanol on cotton swabs (3X). The surgery was performed under a stereomicroscope at ×3–4 magnification. A 1-cm skin incision was made parallel to the body wall in the inguinal area using fine forceps and surgical scissors. The subcutaneous fat pad was bluntly dissected away from the femoral sheath, and then, 7–0 silk ligatures were placed around the femoral artery and vein bundle avoiding the femoral nerve at four sites: distal femoral, perforating artery, epigastric artery, and proximal femoral. Vessels were cut within the ligatures, completely occluding blood flow from the segment of femoral artery and vein between the distal and proximal 7–0 silk knots (Fig. 7). Finally, we sutured the skin closed with 6–0 nylon sutures in a simple interrupted pattern, administered 0.5 ml saline subcutaneously, discontinued anesthesia, and monitored the mouse's recovery on the heating pad.

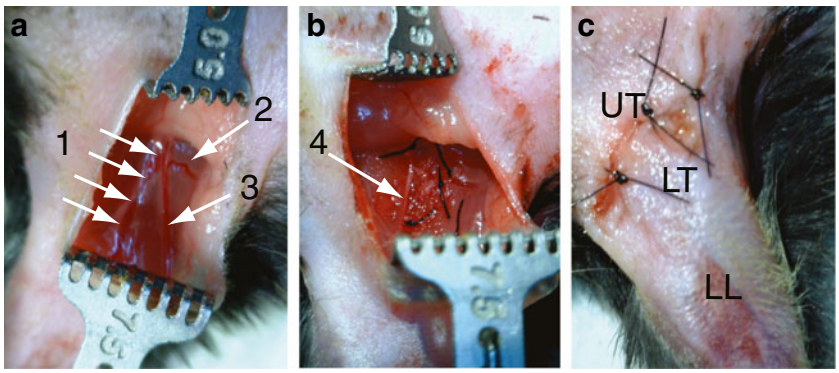

Fig. 7. Pictures of femoral artery and vein resection procedure for the mouse HLI model. **a** Exposure of femoral artery, vein, and nerve complex (*1*), perforating artery (*2*), and epigastric artery (*3*), **b** ligation and resection of blood vessels (*1–3*) without disturbing the femoral nerve (*4*). **c** The skin incision was closed with three simple interrupted sutures over the upper thigh (*UT*). Resection of the femoral artery results in ischemia in the lower thigh (*LT*) and lower limb (*LL*).

Optical Imaging

Imaging studies were conducted at 3 days post-operation. Mice were anesthetized using 2 % isoflurane at 1 L/min. Contrast agents, LS601-PEG_{40} or LS601R-PEG_{40}, were administered intravenously *via* lateral tail vein. Mice were imaged using the Pearl NIR imaging system as described above, immediately post-injection, 1, 4, and 24 h post-injection. After the final scan, anesthetized mice were euthanized *via* cervical dislocation. Thigh and calf muscle from both control and experimental hindlimbs were collected, snap-frozen in OCT, and stored in −80 °C freezer for histological analysis.

Statistical Analysis

Region of interest (ROI) analysis was performed by selecting a thigh region distal to the surgical incision on the NIR fluorescence image, and mean intensity value determined using PearlCam software (LiCor). Mean intensity values for injured and uninjured limbs were compared for each group using Student's *t* test with $\alpha = 0.01$. Statistical analysis of optical imaging data was performed using Graphpad Prism 5.0.

Histology

Specimens from mouse thigh from control and ischemic hindlimbs were fixed in 4 % paraformaldehyde, embedded in paraffin, and cut with cryostat into 5-μm sections for immunohistochemistry using antibodies specific to 8-OHG (oxidized guanosine) and nitrotyrosine.

Acknowledgment. The authors appreciate the help of Susannah Grathwohl to implement the HLI method. This research was supported in part by K01RR026095 (WA) from the National Center for Research Resources, National Cancer Institute R21CA149814 (MB), and National Heart Lung and Blood Institute as a Program of Excellence in Nanotechnology (HHSN268201000046C) (MB). SM was supported by the Mallinckrodt Institute of Radiology Summer Research Program. The pulmonology core is supported by NHLBI P50 HL084922 grant from the NIH (RP).

Conflict of Interest. The authors declare no competing financial interest.

References

1. van der Laan AM, Piek JJ, van Royen N (2009) Targeting angiogenesis to restore the microcirculation after reperfused MI. Nat Rev Cardiol 6:515–523
2. Silvestre JS, Mallat Z, Tedgui A, Levy BI (2008) Post-ischaemic neovascularization and inflammation. Cardiovasc Res 78:242–249
3. Schuster A, Morton G, Chiribiri A et al (2012) Imaging in the management of ischemic cardiomyopathy: special focus on magnetic resonance. J Am Coll Cardiol 59:359–370
4. Ushio-Fukai M, Alexander RW (2004) Reactive oxygen species as mediators of angiogenesis signaling—role of NAD(P)H oxidase. Mol Cell Biochem 264:85–97
5. Hori M, Nishida K (2009) Oxidative stress and left ventricular remodelling after myocardial infarction. Cardiovasc Res 81:457–464
6. Sunderkotter C, Steinbrink K, Goebeler M et al (1994) Macrophages and angiogenesis. J Leukoc Biol 55:410–422
7. Forman HJ, Torres M (2002) Reactive oxygen species and cell signaling: respiratory burst in macrophage signaling. Am J Respir Crit Care Med 166:S4–8
8. Xie L, Lin AS, Kundu K, et al. (2012) Quantitative imaging of cartilage and bone morphology, reactive oxygen species, and vascularization in a rodent model of osteoarthritis. Arthritis and Rheumatism
9. Selvam S, Kundu K, Templeman KL et al (2011) Minimally invasive, longitudinal monitoring of biomaterial-associated inflammation by fluorescence imaging. Biomaterials 32:7785–7792
10. Kundu K, Knight SF, Lee S et al (2010) A significant improvement of the efficacy of radical oxidant probes by the kinetic isotope effect. Angew Chem Int Ed Engl 49:6134–6138
11. Gustafson T, Yan Y, Newton P et al (2012) A NIR dye for development of peripheral nerve targeted probes. Med Chem Comm 3:685–690
12. Gustafson TP, Cao Q, Achilefu S, Berezin MY (2012) Defining a polymethine dye for fluorescence anisotropy applications in the near-infrared spectral range. Chemphyschem: a European journal of chemical physics and physical chemistry
13. Kundu K, Knight SF, Willett N et al (2009) Hydrocyanines: a class of fluorescent sensors that can image reactive oxygen species in cell culture, tissue, and *in vivo*. Angew Chem Int Ed 48:299–303
14. Lakowicz JR (2006) Principles of fluorescence spectroscopy, 3rd edn. Springer, New York
15. Kikuchi K, Nagano T, Hayakawa H et al (1993) Real time measurement of nitric oxide produced *ex vivo* by luminol-H_2O_2 chemiluminescence method. J Biol Chem 268:23106–23110
16. Hellingman AA, Bastiaansen AJ, de Vries MR et al (2010) Variations in surgical procedures for hind limb ischaemia mouse models result in differences in collateral formation. Eur J Vasc Endovasc Surg: Off J Eur Soc Vasc Surg 40:796–803
17. Niiyama H, Huang NF, Rollins MD, Cooke JP (2009) Murine model of hindlimb ischemia. J Vis Exp (23):1035
18. Kim J, Cao L, Shvartsman D et al (2011) Targeted delivery of nanoparticles to ischemic muscle for imaging and therapeutic angiogenesis. Nano Lett 11:694–700
19. Nasongkla N, Chen B, Macaraeg N et al (2009) Dependence of pharmacokinetics and biodistribution on polymer architecture: effect of cyclic versus linear polymers. J Am Chem Soc 131:3842–3843
20. Fox ME, Szoka FC, Frechet JM (2009) Soluble polymer carriers for the treatment of cancer: the importance of molecular architecture. Acc Chem Res 42:1141–1151
21. Liu Y, Bauer AQ, Akers WJ et al (2011) Hands-free, wireless goggles for near-infrared fluorescence and real-time image-guided surgery. Surgery 149:689–698
22. Solomon M, White BR, Nothdruft RE et al (2011) Video-rate fluorescence diffuse optical tomography for *in vivo* sentinel lymph node imaging. Biomed Opt Express 2:3267–3277
23. Kim C, Erpelding TN, Maslov K et al (2010) Handheld array-based photoacoustic probe for guiding needle biopsy of sentinel lymph nodes. J Biomed Opt 15, 046010
24. Benson RC, Kues HA (1978) Fluorescence properties of indocyanine green as related to angiography. Phys Med Biol 23:159–163
25. Berezin MY, Lee H, Akers W, Achilefu S (2007) Near infrared dyes as lifetime solvatochromic probes for micropolarity measurements of biological systems. Biophys J 93:2892–2899
26. Liu Y, Pressly ED, Abendschein DR et al (2011) Targeting angiogenesis using a C-type atrial natriuretic factor-conjugated nanoprobe and PET. J Nucl Med: Off Publ, Soc Nucl Med 52:1956–1963